

SCIENTIFIC REPORTS

OPEN

Surface Plasmon Coupling in GaN:Eu Light Emitters with Metal-Nitrides

Ioannis E. Fragkos & Nelson Tansu

Metal-nitrides of hafnium nitride (HfN), zirconium nitride (ZrN) and titanium nitride (TiN) are investigated as plasmonic materials to enhance the internal quantum efficiency of a GaN:Eu red light emitter. Theoretical calculations are performed to evaluate the surface plasmon polariton dispersion relation and Purcell enhancement factor for a single metal-nitride layer on top of the GaN:Eu emitter. Our findings suggest that among the metal-nitrides investigated in this study, TiN is the most promising candidate for use as plasmonic material to increase the internal quantum efficiency in GaN:Eu red light emitters.

Europium-doped gallium nitride (GaN:Eu) based light emitters have drawn much attention in the field of photonics due to the sharp luminescence of Eu^{+3} ions emitting in the red spectral regime^{1–8}. The recent progress in the GaN:Eu based material has resulted in promising direction for its implementation as a candidate for active region in red light-emitting devices (LEDs)^{9–17}. However, regardless the evolution and the improvements of the GaN:Eu devices over the years, the progress in the electrically-driven devices has been limited to low peak internal quantum efficiency (η_{IQE}) and drooping behavior of external quantum efficiency (η_{EQE}) with increasing current density¹⁷.

In our recent work¹⁸, we developed a current injection efficiency model ($\eta_{injection}$) to understand the governing parameters affecting the internal quantum efficiency and efficiency-droop characteristics in the electrically-driven GaN:Eu LEDs. This model¹⁸ also allows one to reveal the fundamental distinct factors that affect the efficiency characteristics in the optically-pumped and electrically-driven GaN:Eu devices. Through this model¹⁸, we identify that the saturation of the excited Eu^{+3} ions in the GaN host - resulted either by optical excitation or electrical injection in the GaN host - as one of the key factors limiting the peak internal quantum efficiency and droop issue at high injection current level. These limiting factors¹⁸ resulted the low current injection efficiency in electrically-driven GaN:Eu LED, which in turn led to a significant reduction in both its internal and external quantum efficiencies.

In addition, we proposed experimental methods on how to increase the external quantum efficiency of these devices. Our studies¹⁸ pointed out the reduction in the radiative life time of Eu^{+3} ions (τ_{rad}) reduces the saturation issue of the Eu^{+3} ions up to higher current density; such approach enables the ability to achieve high current injection level and minimize the drooping issue at higher current density (for electrically-driven GaN:Eu devices) and at higher photon flux (for optically-excited devices). The reduction in the τ_{rad} also increases the radiative efficiency ($\eta_{radiative}$) of the Eu^{+3} ions, which in turn results in a further enhancement of the internal quantum efficiency ($\eta_{IQE} = \eta_{injection} \cdot \eta_{radiative}$) of the device.

The reduction of the radiative lifetime of Eu^{+3} ions can be physically achieved by using the coupling of the emitted electromagnetic (EM) mode to a surface plasmon (SP) of a conductive layer, spaced at a distance from the emitter, thus creating a surface plasmon polariton (SPP). Through this coupling, the radiative efficiency of the system is enhanced due to increase of photon density states near the surface plasmon energy E_{sp} - a phenomenon known as the Purcell effect¹⁹. It is important to notice that the coupling mechanism of the emitter to the surface plasmons of the conductive layer, usually requires special configurations in order to achieve phase matching conditions of the emitted photon of the light source and the surface plasmon of the conductive layer. However, it has been shown that if the light source is close to the conductive layer within the wavelength scale, a SPP can be generated via direct energy transfer from the light source to the surface plasmon. Therefore, for the case where the

Center for Photonics and Nanoelectronics, Department of Electrical and Computer Engineering, Lehigh University, Bethlehem, PA, 18015, USA. Correspondence and requests for materials should be addressed to I.E.F. (email: iof213@lehigh.edu) or N.T. (email: tansu@lehigh.edu)

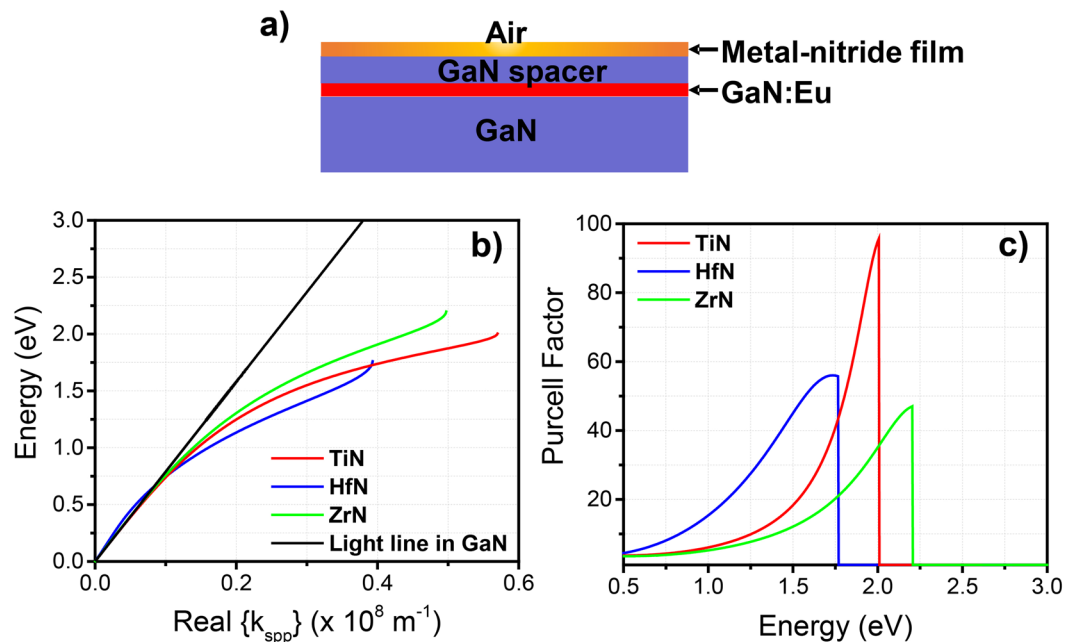


Figure 1. (a) Schematic of the structure used for the simulations. (b) Energy dispersion relation of the surface plasmon polariton (SPP) for different metal-nitrides. The thickness of the metal-nitride film was set at 20 nm while the GaN spacer thickness of was set at 15 nm. (c) Purcell factor for different metal-nitrides films on top of the GaN:Eu red light emitter.

conductive layer is placed on top of a light source in a relatively short distance from it, no special configurations are required to generate SPPs^{20–22}.

The concept of SP coupling to the active materials in III-Nitride semiconductors resulting in an enhanced radiative efficiency has been reported^{23–29}. More specifically, metallic thin layers such as silver (Ag) and gold (Au) have been deposited on top of InGaN multiple quantum wells for increasing the efficiency of the emitter in the ultraviolet (UV) and visible spectral regimes^{23–29}. However, despite the popularity of these noble metals as the metallic plasmonic material choices for applications in the UV and visible spectral regime, such materials are unsuitable for plasmonic applications in the red and near infrared spectral regime attributed to high Ohmic losses^{30,31}. In contrast, the transition-metal nitrides, such as titanium nitride (TiN), hafnium nitride (HfN) and zirconium nitride (ZrN), are promising candidates as low-loss plasmonic materials in the visible and near-IR spectral regimes attributed to the ability for achieving negative real permittivity values at relatively lower carrier concentrations^{32–37}. In addition, these materials offer a wide tunability of their dielectric properties, usually through the variation of the deposition parameters^{32–37}.

In this work, we theoretically investigate the use of metal nitrides - TiN, HfN and ZrN - as plasmonic materials in the red spectral regime. More specifically, we study the effect of the coupling of the surface plasmons of the metal-nitride to the GaN:Eu based red light emitter and its impact on the internal quantum efficiency of this particular type of red light emitter. A comparison among the metal nitrides is made, and is found that TiN is the most suitable selection for applications in the characteristic photon energy of the GaN:Eu emitter at ~ 2 eV. Consequently, the study is proceeded to investigate the effect of the TiN layer thickness (d_{TiN}) and GaN spacer thickness (d_{spr}) on the SPP dispersion relation and Purcell factor. The impact on the electrically-driven device characteristics for TiN-based surface plasmon coupled on GaN:Eu LEDs is also presented.

Simulation Method and Results

For our theoretical investigation we consider the structure depicted in Fig. 1(a). The metal-nitride layer is placed on top of a GaN/GaN:Eu/GaN emitter, where the last layer of GaN serves as the spacer between the GaN:Eu and metal-nitride regions. The SPP dispersion relation is computed by solving the Maxwell equations in the GaN/GaN:Eu/GaN active layer, metal-nitride plasmonic layer, and air region with the appropriate boundary conditions. After solving the SPP dispersion relation, the electric field profile is evaluated to calculate the Purcell enhancement factor; this method is similar to work presented in ref.²³. The simulations are performed assuming the dielectric functions of GaN:Eu and GaN regions as identical and equal to $\epsilon_{r\text{GaN}} = n_{\text{GaN}}^2$, where $n_{\text{GaN}} = 2.5$ is the refractive index of GaN. For the dielectric function of the metal-nitrides, a Drude-Lorentz model is used according to the following formula:

$$\epsilon_{rMN}(\omega) = \epsilon_{\infty} - \frac{\omega_p^2}{\omega^2 - i\omega\Gamma_p} + \sum_{j=1}^m \frac{f_j \omega_j^2}{\omega_j^2 - \omega^2 + i\omega\Gamma_j}$$

Parameter	HfN	TiN	ZrN
ϵ_∞	2.5	4.855	3.465
ω_p [eV]	5.71	7.9308	8.018
Γ_p [eV]	0.6878	0.1795	0.5192
ω_1 [eV]	4.60	4.2196	5.48
f_1	1.20	3.2907	2.4509
Γ_1 [eV]	2.65	2.0341	1.7369
Reference	37	36	36

Table 1. Parameters of the Drude-Lorentz model for the different metal-nitrides investigated in this study.

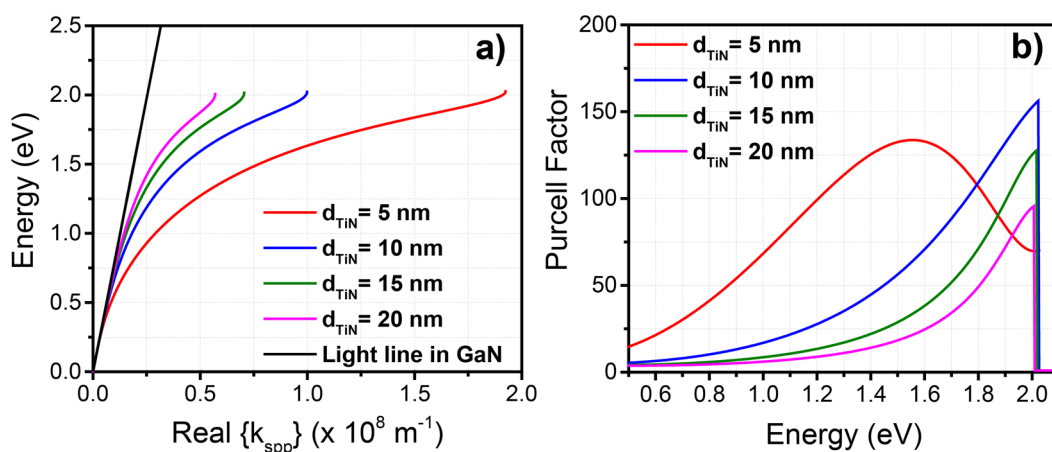


Figure 2. (a) Energy dispersion relation of the surface plasmon polariton (SPP) for different TiN thickness (d_{TiN}) with GaN spacer thickness of $d_{\text{spr}} = 15$ nm. (b) Purcell factor for different TiN thickness (d_{TiN}) with GaN spacer thickness of $d_{\text{spr}} = 15$ nm.

where the ϵ_∞ is the background constant permittivity at high frequency, the ω_p is the plasma frequency of the metal-nitride, the Γ_p is the damping factor, and the ω_j is the frequency of the Lorentz oscillators with strength f_j and damping factor Γ_j . The parameters of the dielectric function of the individual metal-nitride materials investigated in this study are shown in Table 1.

Prior to the theoretical investigation it is important to mention that the structure studied here (Fig. 1(a)) is basically the active region of a GaN:Eu based device. In addition, in our study we have excluded any possible cavity effects on the Purcell enhancement factor. The structure depicted in Fig. 1(a) does not contain any highly reflective layers (i.e. reflective metals, distributed Bragg reflectors), as well as does not meet the criteria for the lowest resonant cavity frequency: the required cavity width for the lowest resonant frequency is $\lambda/2$ (where the λ is the characteristic emitted wavelength of the light source), while the total width of the structure depicted in Fig. 1(a) is much less than the above required condition.

Figure 1(b) depicts the effect of different metal-nitride materials on the SPP dispersion relation. The thickness of the metal-nitride layer was fixed at 20 nm while the thickness of the GaN spacer was fixed at 15 nm. It can be seen that the SPP dispersion relation approaches an asymptotic limit which corresponds to the characteristic surface plasmon polariton energy (E_{sp}). Among the metal-nitrides the energy of the SPP of the TiN is very close to the characteristic photon energy of the GaN:Eu emitter (~ 2 eV) in the red spectral regime. In contrast the ZrN and HfN present a characteristic E_{sp} which is in the green (~ 2.2 eV) and deep red (~ 1.70 eV) spectral regime respectively. In addition, as it is shown in Fig. 1(c), TiN presents high Purcell factor at the characteristic energy of E_{sp} as compared to the other metal-nitrides. It is important to mention that this comparison of metal-nitrides aims on the selection of the appropriate material for plasmonic application only in the spectral regime of the characteristic photon energy of GaN:Eu emitter at ~ 2 eV. Therefore, TiN is found to be a suitable plasmonic material for the surface plasmon coupling with the GaN:Eu based red light emitter. The use of the other metal-nitrides presented in this study can be used for similar applications in the spectral regime of their characteristic asymptotic limit of E_{sp} .

Figure 2(a) depicts the effect of different TiN layer thickness on the SPP dispersion relation for the case of $d_{\text{spr}} = 15$ nm. By decreasing the TiN thickness, the SPP curve is pushed down at lower energies while maintaining the asymptotic limit at $E_{sp} \sim 2.0$ eV. In general, for a thin conductive layer surrounded by dielectrics, collective plasma oscillations localized at the metal/dielectric and metal/air interfaces exist. The thinner the conductive layer is, the stronger the coupling between the SPPs at the two interfaces becomes resulting in a larger energy separation of the two SPPs²⁷. As the energy approaches the E_{sp} , the penetration depth of the electric field of the SPP in the conductive layer significantly reduces resulting in the non-interaction of the two SPPs at the two interfaces. Hence, the limit of E_{sp} is independent of the conductive layer thickness.

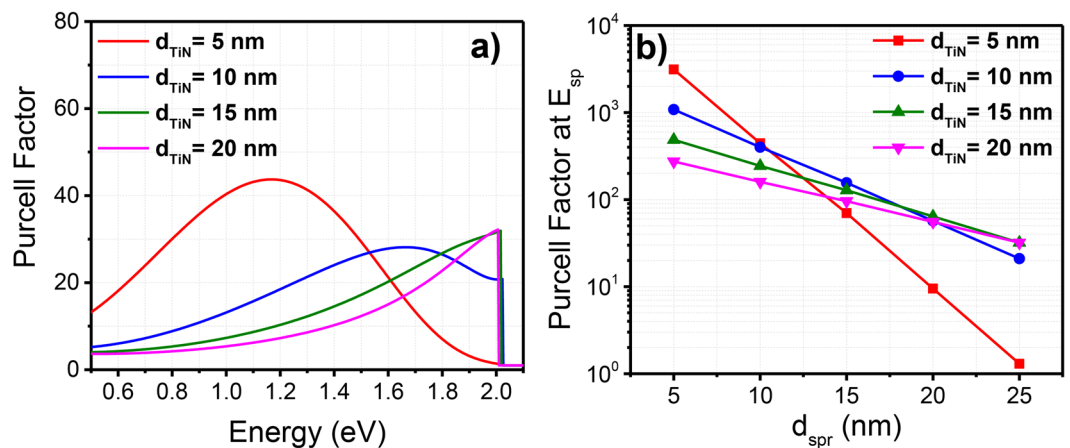


Figure 3. (a) Purcell factor for different TiN thickness (d_{TiN}) with GaN spacer thickness of $d_{spr} = 25$ nm. (b) Purcell factors at the asymptotic limit of E_{sp} versus different GaN spacer thickness (d_{spr}) plotted for different thickness of TiN (d_{TiN}).

Figure 2(b) depicts the Purcell factor for various TiN thicknesses for the case of $d_{spr} = 15$ nm. As the energy of the SPP increases towards E_{sp} , the Purcell factor increases due to the increased surface plasmon density of states (SPDS). The maximum value of the Purcell factor is obtained at the limit of E_{sp} , where the SPDS has its maximum value. Note that the SPDS is proportional to $(dE/dk)^{-1}$ of the dispersion curve shown in Fig. 2(a). At energies above E_{sp} , the GaN/TiN interface cannot support a guided SPP mode, hence the Purcell factor drops to unity. In addition, by decreasing the TiN thickness, the Purcell factor can be obtained for values higher than 100. In contrast, by reducing the TiN thickness beyond 10 nm, the Purcell factor drops at energy $\sim E_{sp}$, while it becomes broader at lower energies. This behavior is attributed to the lower energies of the SPP for the case of $d_{TiN} = 5$ nm as compared to those with $d_{TiN} > 5$ nm, as shown in Fig. 2(a).

As shown in Fig. 2(b), the use of thinner TiN layer results in larger SPP wavevector (k_{spp}) with high Purcell factor; however, such condition comes at the expense of the SPP propagation length (L_{spp}). The propagation length L_{spp} of ~ 4.05 nm is obtained for the case of $d_{TiN} = 5$ nm. As the d_{TiN} is increased to 15 nm (or 20 nm), the L_{spp} increases to ~ 11.7 nm (~ 15 nm). Despite the relatively low propagation length, the out-coupling of the SPP into the air can be achieved through scattering via the roughness of the TiN/GaN interface^{25,38}.

In Fig. 3(a), a similar dependency of the Purcell factor on the TiN thickness is observed for a different spacer thickness of $d_{spr} = 25$ nm. Figure 3(b) depicts the Purcell factors at the asymptotic limit of E_{sp} versus different spacer thickness, plotted for different TiN thicknesses. A reduction of the Purcell factor with the spacer thickness is observed for all cases. In general, a thicker spacer corresponds to a larger separation of the TiN and GaN:Eu layers, which in turn results in a weaker coupling of the GaN:Eu region to the SP layer. The interplay role of the conductive and the spacer layer thicknesses has also been demonstrated for the case of GaN/Ag/air interfaces²⁴.

The dielectric properties of TiN strongly depend on the deposition conditions^{39–45}. By tuning the deposition conditions of TiN on top of GaN, the desirable dielectric properties of TiN can be achieved. In this way the surface plasmon frequency can be designed to cover a wide range of the visible spectral regime. In contrast to the single TiN layer presented in this work, two different layers of TiN with different dielectric functions can be used to tune the asymptotic limit E_{sp} . The concept of a double layer (DL) has been demonstrated for the case of the InGaN QWs where the thickness of the individual layers of the DL varied to tune the surface plasmon energy E_{sp} ^{27,28}. A similar concept can be applied for the case of a double TiN layer on top of GaN based light emitters, including GaN:Eu and InGaN QWs, which could potentially increase the Purcell factor over a wide range in the visible spectral regime.

Impact of Purcell Factor on Internal Quantum Efficiency

The analysis of the Purcell factor in the internal quantum efficiency of the electrically-driven GaN:Eu LEDs is presented in Fig. 4, in order to quantify the improvement presented from the use of surface plasmon structure. The internal quantum efficiency of a GaN/GaN:Eu/GaN device was calculated in a similar approach to ref.⁴⁶. The introduction of surface plasmon coupled active region in GaN:Eu results in an order of magnitude increase in the internal quantum efficiency of the electrically-driven devices, and provides a reduction of efficiency-droop up to relatively high current density (J).

A large surface plasmon coupled structure (Purcell factor ~ 1000) results in peak internal quantum efficiency $\sim 20\%$ for $J = 0.1$ A/cm². The droop suppression from the Purcell effect is found to be more significant at higher current densities. Specifically, a Purcell factor of 1000 results in an increase of the internal quantum efficiency by ~ 16 times at a current density of $J = 10$ A/cm², while the same Purcell factor results in only ~ 1.7 times higher improvement for $J = 0.1$ A/cm². For the structure without any surface plasmon coupling (reference case, with Purcell factor = 1), a significant reduction (~ 30 times) in the internal quantum efficiency is observed as the current density increases from $J = 0.1$ A/cm² to $J = 10$ A/cm². In contrast, the reduction of only ~ 3.5 times in the internal quantum efficiency was observed in the structure having a large Purcell factor (~ 1000) for the same current density range ($J = 0.1$ A/cm² to $J = 10$ A/cm²). As mentioned earlier, the changes in the Purcell factor

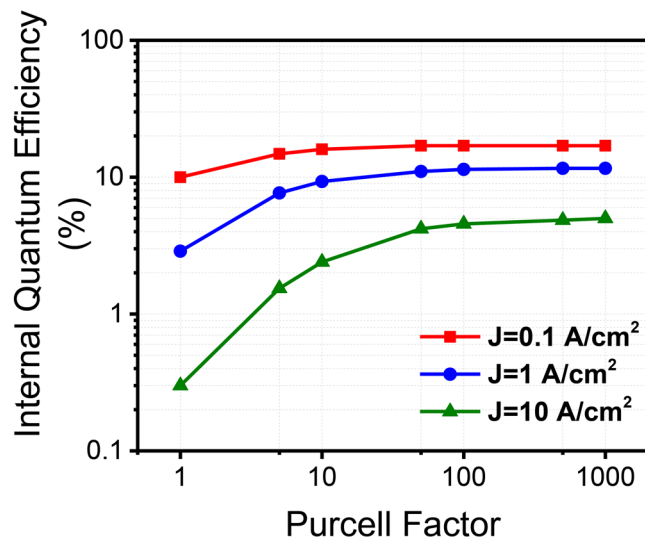


Figure 4. Internal quantum efficiencies of electrically-driven GaN:Eu LED taking into consideration current injection efficiency as a function on Purcell enhancement factor plotted for three different current densities (J).

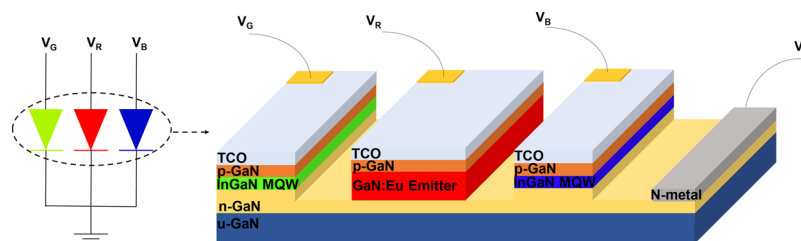


Figure 5. Concept of monolithically integrated white LED based on GaN material. The high efficiency blue and green InGaN QW can be monolithically integrated with the high efficiency red GaN:Eu emitter.

correspond in changes of the radiative lifetime of the GaN:Eu region (i.e Eu^{+3} ions) which affect the radiative efficiency of the system. In addition, a change in the current injection efficiency will also occur resulting in an overall change of the internal quantum efficiency of the GaN:Eu device.

In addition to the need to achieve high internal quantum efficiency in the electrically-injected surface-plasmon GaN:Eu LED, numerous approaches for achieving high extraction efficiency needs to be considered. The metal-nitrides and other surface plasmon metals have surface roughness of ~ 1 nm via evaporation or sputtering^{25,28,35,38}, and such roughness contributes greatly to the light scattering into and out of the surface plasmon layer. It is expected that the use of thin-film flip-chip (TFFC) LEDs can be implemented in surface-plasmon structure for enabling extraction in the order of $\sim 75\%$ or higher^{47–49}. The advantage presented in this work by using surface plasmon coupling to increase the IQE in the electrically-injected GaN:Eu LED can be incorporated in the TFFC configuration.

The development for high efficiency red light emitters based on GaN:Eu or $\text{In}_x\text{Ga}_{1-x}\text{N}$ QW active region, is mandatory for the monolithic realization of GaN-based white LEDs. The solutions for challenges to achieve InGaN-based red emitters are important and still being pursued. However, the use of GaN:Eu LEDs may provide an interesting advantage over InGaN, namely: i) narrower linewidth red spectral emission, and ii) less temperature-sensitivity to the emission wavelength^{10–13,17,50,51}. The availability of red emitters based on GaN:Eu LEDs provides a pathway for integration with the more established InGaN-based blue and green emitters. Figure 5 shows the integration method that can be pursued for GaN-based display emitters with integration of InGaN-based LEDs and red-emitters based on GaN:Eu materials. Such integration can provide a solution for individually-addressed emitter in the three colors grown by selective-area epitaxy.

Conclusions

The metal-nitrides of hafnium-nitride (HfN), zirconium nitride (ZrN) and titanium nitride (TiN) have been investigated as plasmonic materials to enhance the internal quantum efficiency of the GaN:Eu red light emitter. It was found that among those metal-nitrides, the TiN is the most promising material candidate for surface plasmon coupling to the GaN:Eu red light emitter. Through the tuning of the TiN and GaN spacer thickness, Purcell factors as high as 1000 can be achieved at a photon energy $\sim E_{sp}$. The coupling of the active region of a GaN:Eu LED to the surface plasmon of the TiN layer is expected to result in significant increase in the internal quantum efficiency of the electrically-driven devices. This approach will provide a pathway for achieving 20% internal quantum

efficiency in electrically-driven devices. A significant reduction in drooping at high current density is expected in the surface-plasmon coupled GaN:Eu electrically-driven LED. The droop suppression in the electrically-driven surface plasmon coupled device is expected to improve by ~16 times over that of the reference devices without employing surface plasmon coupling.

References

- Heikenfeld, J., Garter, M., Lee, D. S., Birkhahn, R. & Steckl, A. J. Red light emission by photoluminescence and electroluminescence from Eu-doped GaN. *Appl. Phys. Lett.* **75**, 1189 (1999).
- Lozykowski, H. J., Jadwisieniczak, W. M., Han, J. & Brown, I. G. Luminescence properties of GaN and Al_{0.14}Ga_{0.86}N/GaN superlattice doped with europium. *Appl. Phys. Lett.* **77**, 767 (2000).
- Kenyon, A. J. Recent developments in rare-earth doped materials for optoelectronics. *Progress in Quantum Elect.* **26**, 225–284 (2002).
- Hömmrich, U. *et al.* Photoluminescence studies of rare earth (Er, Eu, Tm) *in situ* doped GaN. *Mat. Sc. Eng. B* **105**, 91–96 (2003).
- Kim, J. H. & Holloway, P. H. Room-temperature photoluminescence and electroluminescence properties of sputter grown gallium nitride doped with europium. *J. Appl. Phys.* **95**, 4787 (2004).
- Sawahata, J., Bang, H., Seo, J. & Akimoto, K. Optical processes of red emission from Eu doped GaN. *Sc. Tech. Adv. Mat.* **6**, 644–648 (2005).
- Wakamatsu, R. *et al.* Luminescence Properties of Eu-Doped GaN Grown on GaN Substrate. *Jap. J. Appl. Phys.* **52**, 08JM03 (2013).
- M. de Boer, W. D. A. *et al.* Optical excitation and external photoluminescence quantum efficiency of Eu³⁺ in GaN. *Sci. Rep.* **4**, 5235 (2014).
- Park, J. H. & Steckl, A. J. Laser action in Eu-doped GaN thin-film cavity at room temperature. *Appl. Phys. Lett.* **85**, 4588 (2004).
- Nishikawa, A., Kawasaki, T., Furukawa, N., Terai, Y. & Fujiwara, Y. Room-temperature red emission from a p-type/europium-doped/n-type gallium nitride light-emitting diode under current injection. *Appl. Phys. Express.* **2**, 071004 (2009).
- Nishikawa, A., Kawasaki, T., Furukawa, N., Terai, Y. & Fujiwara, Y. Electroluminescence properties of Eu-doped GaN-based red light-emitting diode by OMVPE. *Phys. Stat. Sol. A* **207**, 1397–1399 (2010).
- Nishikawa, A., Furukawa, N., Kawasaki, T., Terai, Y. & Fujiwara, Y. Improved luminescence properties of Eu-doped GaN light emitting diodes grown by atmospheric-pressure organometallic vapor phase epitaxy. *Appl. Phys. Lett.* **97**, 051113 (2010).
- Nishikawa, A., Furukawa, N., Kawasaki, T., Terai, Y. & Fujiwara, Y. Room-temperature red emission from light-emitting diodes with Eu-doped GaN grown by organometallic vapor phase epitaxy. *Optical Mat.* **33**, 1071–1074 (2011).
- Sekiguchi, H. *et al.* Red light-emitting diodes with site-selective Eu-doped GaN active layer. *Jap. J. Appl. Phys.* **52**, 08JH01 (2013).
- Ishii, M., Koizumi, A. & Fujiwara, Y. Nanoscale determinant to brighten up GaN:Eu red light-emitting diode: Local potential of Eud defect complexes. *J. Appl. Phys.* **117**, 155307 (2015).
- Arai, T. *et al.* Enhanced excitation efficiency of Eu ions in Eu-doped GaN/AlGaIn multiple quantum well structures grown by organometallic vapor phase epitaxy. *J. Luminescence* **158**, 70–74 (2015).
- Zhu, W. *et al.* High-power Eu-doped GaN red LED based on a multilayer structure grown at lower temperatures by organometallic vapor phase epitaxy. *MRS Adv.* **67**, 159–164 (2017).
- Fragkos, I. E., Tan, C. K., Dierolf, V., Fujiwara, Y. & Tansu, N. Pathway towards high-efficiency Eu-doped GaN light emitting diodes. *Sci. Rep.* **7**, 1468 (2017).
- Purcell, E. M. Spontaneous emission probabilities at radio frequencies. *Phys. Rev.* **69**, 681 (1946).
- Barnes, W. L. Electromagnetic crystals for surface plasmon polaritons and the extraction of light from emissive devices. *J. of Lightwave Tech.* **17**, 11 (1999).
- Nomura, W., Ohtsu, M. & Yatsui, T. Nanodot coupler with a surface plasmon polariton condenser for optical far/near-field conversion. *Appl. Phys. Lett.* **86**, 181108 (2005).
- Wang, Z. M. & Neogi, A. *Nanoscale Photonics and Optoelectronics, Lecture Notes in Nanoscale Science and Technology 9*, Springer Science + Business Media, LLC (2010)
- Gontijo, M. *et al.* Coupling of InGaIn quantum-well photoluminescence to silver surface plasmons. *Phys. Rev. B* **60**, 11564 (1999).
- Neogi, A. *et al.* Enhancement of spontaneous emission in a quantum well by resonant surface plasmon coupling. *Phys. Rev. B* **66**, 153305 (2002).
- Okamoto, K. *et al.* Surface plasmon-enhanced light emitters based on InGaIn quantum wells. *Nature Mater.* **3**, 601–605 (2004).
- Okamoto, K. *et al.* Surface plasmon enhanced spontaneous emission rate of InGaIn/GaN quantum wells probed by time-resolved photoluminescence spectroscopy. *Appl. Phys. Lett.* **87**, 071102 (2005).
- Paiella, R. Tunable surface plasmons in coupled metallo-dielectric multiple layers for light emission efficiency enhancement. *Appl. Phys. Lett.* **87**, 111104 (2005).
- Zhao, H. P., Zhang, J., Liu, G. Y. & Tansu, N. Surface plasmon dispersion engineering via double metallic Au/Ag layers for III-nitride based light-emitting diodes. *Appl. Phys. Lett.* **98**, 151115 (2011).
- Lin, J. *et al.* Surface plasmon enhanced UV emission in AlGaIn/GaN quantum well. *Appl. Phys. Lett.* **97**, 221104 (2010).
- Johnson, P. B. & Christy, R. W. Optical constants of the noble metals. *Phys. Rev. B* **6**, 4370 (1972).
- West, P. R. *et al.* Searching for better plasmonic materials. *Laser Photonics Rev.* **4**, 795 (2010).
- Steinmüller-Nethl, D., Kovacs, R., Gornik, E. & Rödhammer, P. Excitation of surface plasmons on titanium nitride films: determination of the dielectric function. *Thin Solid Films* **237**, 277–281 (1994).
- Hibbins, A. P., Sambles, J. R. & Lawrence, C. R. Surface plasmon-polariton study of the optical dielectric function of titanium nitride. *J. Mod. Opt.* **45**, 2051–2062 (1994).
- Chen, N. C. *et al.* Excitation of surface plasma wave at TiN/air interface in the Kretschmann geometry. *J. Appl. Phys.* **109**, 043104 (2011).
- Naik, V. *et al.* Titanium nitride as a plasmonic material for visible and near-infrared wavelengths. *Opt. Mat. Exp.* **4**, 478–489 (2012).
- Naik, V. G., Shalev, V. M. & Botlasheva, A. Alternative plasmonic materials: beyond gold and silver. *Adv. Mater.* **25**, 3264–3294 (2013).
- Gu, Z. *et al.* Optical reflectivity and hardness improvement of hafnium nitride films via tantalum alloying. *Appl. Phys. Lett.* **109**, 232102 (2016).
- Barnes, W. L. Light-emitting devices: Turning the tables on surface plasmons. *Nature Mater.* **3**, 588–589 (2004).
- Wiemer, C., Lévy, F. & Bussy, F. Determination of chemical composition and its relationship with optical properties of Ti-N and Ti-V-N sputtered thin films. *Surf. Coat. Technol.* **68**, 181–187 (1994).
- Humlíček, J. *et al.* Ellipsometry and transport studies of thin-film metal nitrides. *Thin Solid Films* **332**, 25–29 (1998).
- Patsalas, P. & Logothetidis, S. Optical, electronic, and transport properties of nanocrystalline titanium nitride thin films. *J. Appl. Phys.* **90**, 4725–4734 (2001).
- Postava, K., Aoyama, M. & Yamaguchi, T. Optical characterization of TiN/SiO₂(1000 nm)/Si system by spectroscopic ellipsometry and reflectometry. *Appl. Surf. Sci.* **175**, 270–275 (2001).
- Huber, P., Manova, D., Mändl, S. & Rauschenbach, B. Optical characterization of TiN produced by metal-plasma immersion ion implantation. *Surf. Coat. Technol.* **142**, 418–423 (2001).

44. Naik, G. V., Kim, J. & Boltasseva, J. Oxides and nitrides as alternatives plasmonic materials in the optical range. *Opt. Mat. Exp.* **1**, 1090 (2011).
45. Patsalas, P., Kalfagiannis, N. & Kassavetis, S. Optical properties and plasmonic performance of titanium nitride. *Materials* **8**, 3128–3154 (2015).
46. Fragkos, I. E., Dierolf, V., Fujiwara, Y. & Tansu, N. Physics of Efficiency Droop in GaN:Eu Light-Emitting Diodes. *Sci. Rep.* **7**, 16773 (2017).
47. Zhu, P. F. & Tansu, N. Resonant cavity effect optimization of III-nitride thin-film flip-chip light-emitting diodes with microsphere arrays. *Applied Optics*. **54**, 20 (2015).
48. Shchekin, O. B. *et al.* High performance thin-film flip-chip InGaN–GaN light-emitting diodes. *Appl. Phys. Lett.* **89**, 071109 (2006).
49. Wierer, J. J. *et al.* High-power AlGaInN flip-chip light-emitting diodes. *Appl. Phys. Lett.* **78**, 3379 (2001).
50. Ohkawa, K., Watanabe, T., Sakamoto, M., Hirako, A. & Deura, M. 740-nm emission from InGaN-based LEDs on c-plane sapphire substrates by MOVPE. *J. Cryst. Growth* **343**, 13 (2012).
51. Hwang, J., Hashimoto, R., Saito, S. & Nunoue, S. Development of InGaN-based red LED grown on (0001) polar surface. *Appl. Phys. Express* **7**, 071003 (2014).

Acknowledgements

This work was supported by US National Science Foundation (ECCS 1408051 and DMR 1505122), and the Daniel E. '39 and Patricia M. Smith Endowed Chair Professorship Fund.

Author Contributions

I.E.F. and N.T. contributed to the discussions, concept development, theoretical analysis, analysis of the results, and writing of the manuscript. N.T. supervised the studies performed in the manuscript.

Additional Information

Competing Interests: The authors declare no competing interests.

Publisher's note: Springer Nature remains neutral with regard to jurisdictional claims in published maps and institutional affiliations.



Open Access This article is licensed under a Creative Commons Attribution 4.0 International License, which permits use, sharing, adaptation, distribution and reproduction in any medium or format, as long as you give appropriate credit to the original author(s) and the source, provide a link to the Creative Commons license, and indicate if changes were made. The images or other third party material in this article are included in the article's Creative Commons license, unless indicated otherwise in a credit line to the material. If material is not included in the article's Creative Commons license and your intended use is not permitted by statutory regulation or exceeds the permitted use, you will need to obtain permission directly from the copyright holder. To view a copy of this license, visit <http://creativecommons.org/licenses/by/4.0/>.

© The Author(s) 2018